Pergamon

0042-6989(94)00177-4

Vision Res. Vol. 35, No. 7, pp. 949–960, 1995

0042-6989/95 $9.50 + 0.00

On the Accuracy of Surface Reconstruction from Disparity Interpolation

YUEDE YANG,* RANDOLPH BLAKE*

Received 9 December 1993; in revised form 25 July 1994

Observers viewed flashed random-dot stereograms depicting a pair of long, narrow, curved ribbons of textured surface defined by a Gabor function in disparity. Observers judged the location of the peak of the depth profile of one ribbon relative to that of the other. In one ribbon, disparity changed smoothly while in the other disparity was periodically sampled. Up to a limiting sampling period, disparity interpolation produced accurate surface reconstruction, but beyond that performance deteriorated rapidly. This interpolation limit depended on surface orientation (vertical vs horizontal) and disparity sign, but not Gabor spatial frequency.

Stereopsis Disparity interpolation Vernier acuity

INTRODUCTION

Textbook accounts of stereopsis often focus on its importance in judging depth. While not incorrect, this emphasis seriously underestimates stereopsis' contribution to vision. Besides depth, stereopsis also can precisely specify the shapes and surface structure of objects in the visual environment. This aspect of stereopsis is most remarkably evidenced in random-dot stereograms (RDSs), where disparity information alone can depict continuous, smooth surfaces of complex objects including cylinders, spirals and saddles (Julesz, 1971; Rogers & Graham, 1983). Equally remarkable, this process of surface representation from disparity can be achieved even when the markings defining the surface are extremely sparse; some of the stereograms of Julesz (1971) yield vivid impressions of surfaces with dot densities as little as 5% (see also Fox & Oross, 1988). The accurate representation of surface properties from sparse disparity samples implicates interpolation processes in human stereopsis. (By interpolation, we mean the specification of a continuous surface fit through a limited set of visible surface markings.) Studies of stereo-interpolation can shed light on the nature of the mechanism of three-dimensional surface reconstruction: although disparity is explicitly represented only at the locations of edges, the binocular nervous system evidently registers those explicit disparities in a manner that affords the recovery of more complete surface information.

The problem of disparity interpolation has received increasing attention recently, in part because of the challenge it poses for current models of stereopsis. It is worth noting, too, that stimulus conditions promoting disparity interpolation occur in the natural environment. These include viewing more distant objects (e.g. trees) through semitransparent materials (e.g. a dirty window) and grouping neighboring figural elements (e.g. a cluster of brown spots) into a coherent whole (e.g. a motionless leopard). Disparity interpolation is also probably related to other stereo-phenomena involving interactions among neighboring elements, phenomena including depth averaging (Parker & Yang, 1989), repulsion/attraction (Westheimer, 1986) and disparity propagation (Mitchison & McKee, 1987a, b). We shall return to the similarities among these phenomena in the Discussion.

In the present study, we explore the accuracy with which a stereoscopically defined surface is represented when that representation requires disparity interpolation. In particular, we have measured the ability of human observers to judge the relative locations of regions of three-dimensional surfaces defined solely by retinal disparity (i.e. surfaces depicted in RDS), including conditions where that disparity information is discontinuous (i.e. conditions where explicit disparity values are discretely sampled over space).† Our motive was to learn what conditions influence disparity interpolation, with an eye toward eventually developing a neural model of this process. For test stimuli, we used RDS depicting surfaces curved in depth. Each surface comprised a strip of dots whose depth profile conformed to a Gabor function (see Figs 1 and 2). In fact, the display looked like a black-and-white textured "ribbon" curved in depth, with the depth undulations defined by a Gabor profile. The peak of the Gabor profile corresponded to the point along the ribbon at which it was

*Department of Psychology, Vanderbilt University, Nashville, TN 37240, U.S.A. [*Email* yangy@ctrvax.vanderbilt.edu].

†This vernier task, in which one stimulus is sampled and another is continuous, is comparable to one devised by Morgan and Watt (1982). In their study, however, test stimuli were defined by luminance, not by disparity as in our study.

nearest (crossed disparity) or farthest (uncrossed disparity) in depth. On individual trials, the observer viewed a pair of these stereoscopic ribbons, one next to the other, and judged the relative position of the depth peak (which is, of course, defined solely by disparity). We term this a stereoscopic vernier acuity task, since the observer is judging the relative alignment of two features defined solely by stereopsis, not by luminance information as in a conventional vernier task. A given ribbon could be defined either by disparities that varied smoothly and continuously (within resolution limits of the display monitor) or by disparities that were periodic, discrete samples from the continuous distribution of disparities. For the periodically sampled ribbon, the periodicity of the disparity sampling was varied from values yielding the impression of a continuous, smooth surface to values yielding the impression of coarsely "scissored" ribbon. The center spatial frequency of the Gabor profile was varied, which in this context corresponded to different rates of curvature in depth (not to luminance variation over space). Note that this manipulation does not alter the depth disparity of the ribbon (i.e. the amount of depth portrayed) but rather the two-dimensional spatial extent of the modulations in depth. We tested with both horizontal and vertical Gabor ribbons, to look for anisotropies in disparity interpolation. It should be stressed that successful performance on this task requires the reconstruction of a complete surface from its sampled disparity values, a point elaborated in the Discussion.

METHODS

Stimuli

Pairs of stereoscopic stimuli in the form of random-dot half-images were generated on a Radius gray scale monitor (P104 phosphor; 1152 × 882 resolution; 72 Hz

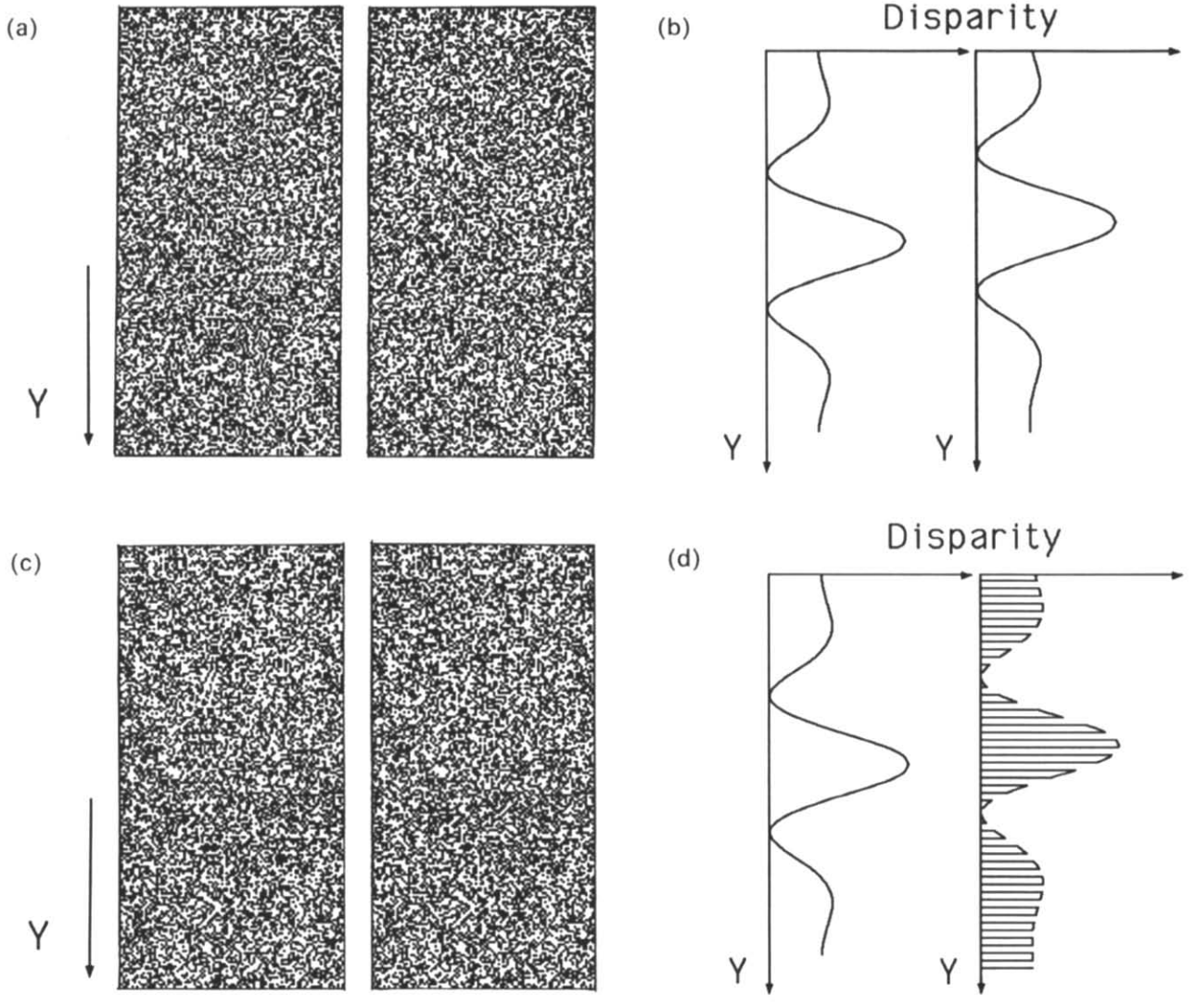

FIGURE 1. Stereo-pair depicting two vertically oriented Gabor ribbons which, when viewed with crossed-eyes, are imaged with crossed disparity. (a). In both three-dimensional ribbons, disparity varies smoothly (within the 1 pixel resolution of disparity available to us). (b). Diagrams of disparity profiles of ribbons in (a) (the small, discrete steps in disparity constituting the actual display are not shown). (c) In the left-hand ribbon ("standard") disparity varies smoothly, while in the right-hand ribbon ("test") disparity is periodically sampled. When viewed from 7× the height of the picture the sampling period of the right-hand ribbon in (c) is approximately 8 min arc. (d). Diagrams of disparity profiles of ribbons in (c).

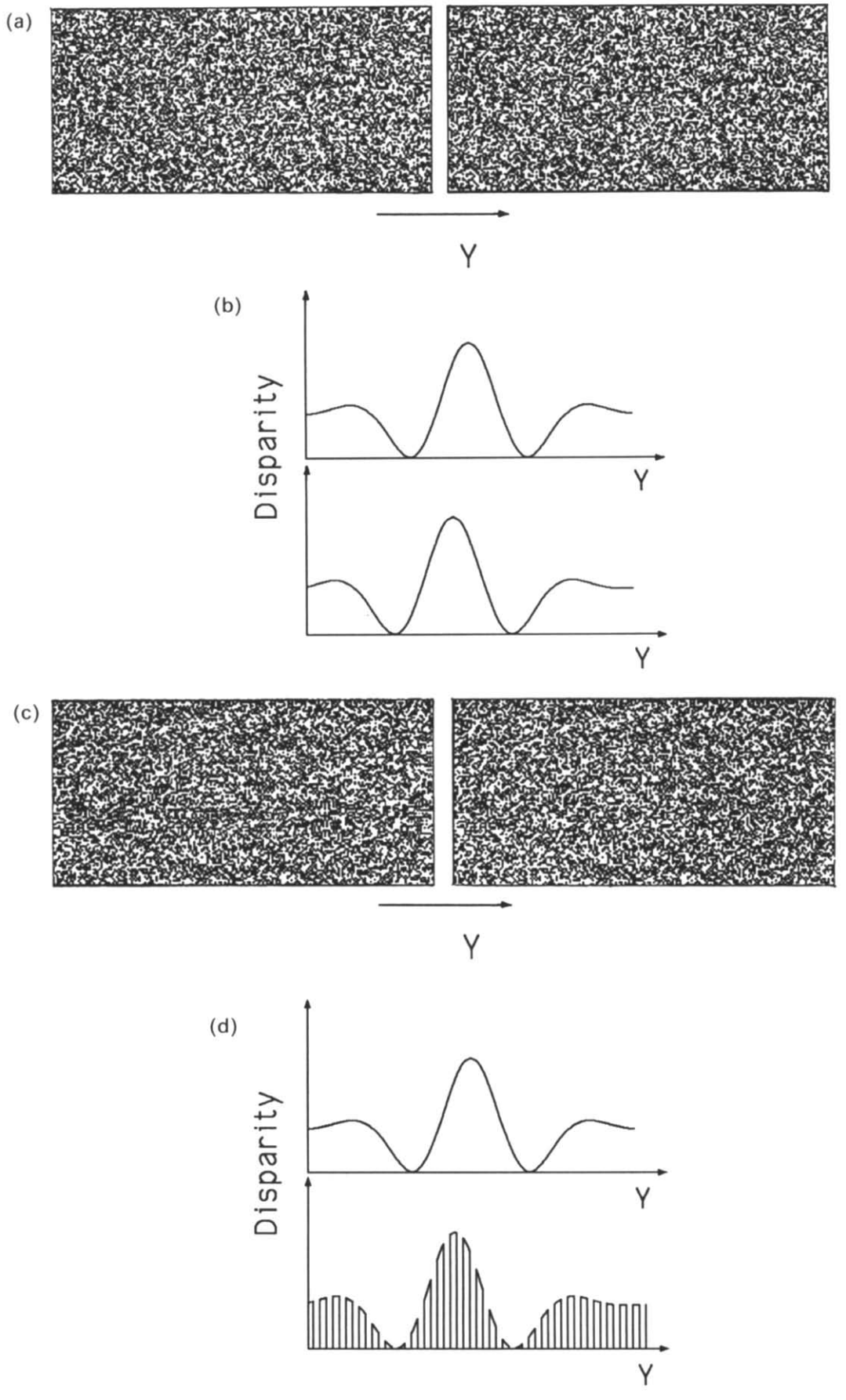

FIGURE 2. Stereo-pair depicting two horizontally oriented Gabor ribbons which, when viewed with crossed-eyes, are imaged with crossed disparity. (a). In both three-dimensional ribbons, disparity varies smoothly. (b). Diagrams of disparity profiles of ribbons in (a). (c) In the top ribbon ("standard") disparity varies smoothly, while in the bottom ribbon ("test") disparity is periodically sampled. When viewed from 7× the width of the picture the sampling period of the bottom ribbon in (c) is approximately 8 min arc. (d). Diagrams of disparity profiles of ribbons in (c).

frame rate) controlled by a Macintosh IIX computer. The two half-images of any given RDS pairs were presented separately to the two eyes through a mirror stereoscope at a viewing distance of 1.07 m.

Examples of stimuli are shown in Figs 1 and 2. Each half-image subtended 3.33 × 6.66 deg and consisted of 20,000 black and white dots (each 2 × 2 pixels, or 2 × 2 min arc), with dot density equaling 50%. The luminance of the white regions was 74 cd m^{-2} and the luminance of the black portions was 0.17 cd m^{-2}. For any given pair of half-images, two ribbons of modulated depth were created by shifting the dots in one eye's view relative to the corresponding dots in the other eye's view. In one set of conditions (termed "vertical"), the long side of the half-images was oriented vertically [Fig. 1 (a, c)] and in another set of conditions ("horizontal") the half-images were longer in the horizontal direction [Fig. 2 (a, c)]. For either set of conditions, the width of a stereoscopic Gabor ribbon was 40 min arc, and the lateral separation between each pair of ribbons was 20 min arc. The length of the ribbons varied with the center frequency of the Gabor profile (i.e. the spatial frequency of the modulation in depth). For any given condition, both Gabor ribbons had the same spatial frequency, which was either 0.185, 0.375 or 0.75 c/deg. (The higher the center frequency of the Gabor function, the greater the rate of change in curvature over space; the ribbon looked more compressed.) Space constant was 0.78 of the reciprocal of the center spatial frequency of the Gabor, which yielded a bandwidth of 1.0 octave. Regardless of center frequency, the peak disparity was always 14 min arc; in some conditions this disparity was crossed (such that the three-dimensional ribbon appeared to float in front of the background) and in others it was uncrossed (such that the three-dimensional ribbon appeared to recede behind the background). For the "vertical" conditions, the disparate region was generated simply by displacing appropriate dots in one eye's view laterally by an amount sufficient to produce the necessary disparity (which varied according to a Gabor profile over the vertical length of the ribbon); the regions vacated by the shifted dots were occupied by the old, unshifted dots.* For the "horizontal" conditions, the depth modulation was produced by varying dot spacing horizontally to produce the required magnitude of disparity specified by a Gabor profile of given center frequency.

In some conditions, the disparity of both members of the pair of three-dimensional ribbons varied "smoothly", meaning that changes in disparity over space were made to within a resolution of 1 min arc, the minimum obtainable with our 2 × 2 pixel dots [see Figs 1(b) and 2(b)]. The curvature in these unsampled three-dimensional ribbons appeared smooth. In other conditions [see Figs 1(d) and 2(d)], disparity in the *standard* strip (the left-hand strip for the vertical conditions; the top strip for the horizontal conditions) changed smoothly while the disparity in the *test* strip (the right-hand strip for the vertical conditions; the bottom strip for the horizontal conditions) consisted of sampled bands of disparate dots (whose disparity conformed to a Gabor function) periodically interspersed by regions of dots imaged with zero disparity. The angular subtense of the disparate samples remained constant at 4 min arc, while the subtense of the zero disparity regions varied from 4 to 28 min arc. Thus, the sampling period varied from 8 to 32 min arc. As sampling period increases, the total percentage of the Gabor ribbon explicitly represented by disparate dots decreases. The sampled bands of disparate dots (i.e. where the surface was specified explicitly) were spatially "anchored" (i.e. always appeared at the same location in the display) regardless of the position of the sampled Gabor envelope. An example of a sampled ribbon is shown in Figs 1(c) and 2(c); in these two examples, the sampling period is 8 min arc (when the figure is viewed at approximately 7 × the length of the longer side of one half-image).

When the RDS stimuli were not present, the two halves of the monitor displayed a fixation target consisting of four binocular brackets and a pair of vertical nonius lines centered within the brackets. The black brackets subtended 1 × 1 deg, and the black nonius lines were 12 min arc.

Observers

Two observers participated in these experiments, one of the authors (YY) and an undergraduate student naive about the purpose of the experiments. Both observers have normal or corrected-to-normal visual acuity and good stereoscopic acuity.

Procedure

For each pair of three-dimensional ribbons, the observer judged whether the depth peak in the test ribbon (i.e. the right-hand ribbon for the vertical conditions, or the bottom ribbon for the horizontal conditions) was above or below (or to the left or right) the peak in the standard. Keep in mind that the peak corresponds to a point of maximum curvature in the Gabor ribbon. Each trial consisted of the following sequence of events.

Initially, the observer adjusted the mirrors of the stereoscope so that the fixation targets were in stable binocular alignment; a cover/uncover test was used to align the mirrors. On each trial, the observer waited until the nonius lines were perfectly aligned and then pressed a key triggering the 167 msec presentation of a RDS stimulus; this brief presentation was followed immediately by a blank, white field. The RDS half-images appeared centered on the location previously occupied

*This stereogram generation technique, in which dots near the depth edges could match either the Gabor ribbon or the zero disparity background, yields an interesting side effect: when the eyes converge such that the background is imaged with zero disparity the ribbon appears narrower than when convergence brings the ribbon itself to zero disparity. The reader may experience upon inspecting Fig. 1(a) or (c). In our experiments, however, exposure duration was too brief to allow convergence to change in this way.

by the fixation marks, which centered the observer's fixation midway between the two three-dimensional ribbons. Following each RDS presentation, the observer used keyboard responses to indicate whether the depth peak of the test strip was above or below (vertical conditions) the depth peak of the standard strip, or whether it was to the left or to the right (horizontal condition) of the depth peak of the standard strip. Following each response, for which there was no feedback, the fixation target reappeared signaling the availability of the next trial. For any given block of trials, the same condition (orientation, sampling period, center frequency, disparity sign) was tested in blocks of 140 trials. Within that block of trials, the location of the peak in depth of the test ribbon was located at one of seven positions relative to the peak of the standard ribbon, with the particular location randomized over trials. The seven peak positions were ± 12 min arc in 4 min arc steps, including zero (i.e. perfect alignment of the peaks). Each of the seven peak locations appeared 20 times within a block of trials. To eliminate absolute positional cues, the location of the peak of the standard ribbon was also varied randomly over trials within the range ± 2 min arc. It is important to remember that, with the sampled Gabor surfaces, the samples of explicit disparity always appeared at the same locations within the display. It was the Gabor envelope of disparity that was shifted from trial to trial, to vary the location of the peak (which sometimes was not explicitly represented in the sampled surface). In other words, any given location of the Gabor surface could be represented by different disparity values (including zero) from trial to trial, depending on the location of the peak of the Gabor profile. Thus, the observer could not simply find the location of the largest disparity actually represented in the sampled display and utilize that information for her judgment. Nor did the observer simply compare the depth of a given sample to the depth at the same spatial location of the adjacent standard. It is easy to show that this strategy would produce non-monotonicities in the psychometric function, which we did not observe. With these sampled disparities and brief exposures, the judgement required interpolating the surface shape and discovering the implicit location of the depth peak. (We stress the depth peak as the key feature on the interpolated surface, because the observer's vernier task was to compare the position of this peak to that of the peak of the unsampled Gabor ribbon; because of our brief exposure durations and the central location of the fixation cross, the observer did not have time to scrutinize various other locations along the surface, such as troughs in the Gabor surface.)

Each block of trials was repeated twice, meaning that 40 observations were collected for each of the seven peak offset values for each condition.

RESULTS

In all instances, we were interested in the accuracy with which observers can judge the position of the depth peak (i.e. point of maximum curvature) in one surface (i.e. Gabor ribbon) relative to another, especially under conditions where the disparity values specifying the surface were sampled, not continuous. Because the task entailed judging the direction of displacement of one depth peak relative to another, we characterize it stereoscopic vernier acuity: vernier, in the sense that spatial offset is the relevant cue, and stereoscopic, in that the requisite information is defined solely by disparity. To reiterate, *stereoscopic vernier acuity* (SVA) is defined as the smallest discriminable offset between two peaks of neighboring three-dimensional surfaces.

To index SVA, we employed the following procedure. Data for each condition (i.e. for each combination of disparity sign/sampling period/center spatial frequency) were plotted as psychometric functions. In principle, performance values should range from 0% to 100%, with the 50% point corresponding to zero offset of the two peaks. The slopes of these functions indicate the ease with which observers were able to discriminate peak offsets: steep slopes indicate high discriminability (i.e. small peak offsets were accurately discriminated) while shallower slopes indicate increasingly poor discriminability. Two examples of the resulting psychometric functions are shown in Fig. 3, one showing rather accurate performance and the other poorer performance. For each psychometric function, we calculated the best-fit probit line and derived that line's slope and took its reciprocal as the index of SVA. (The reciprocal of slope is equivalent to the standard deviation of the

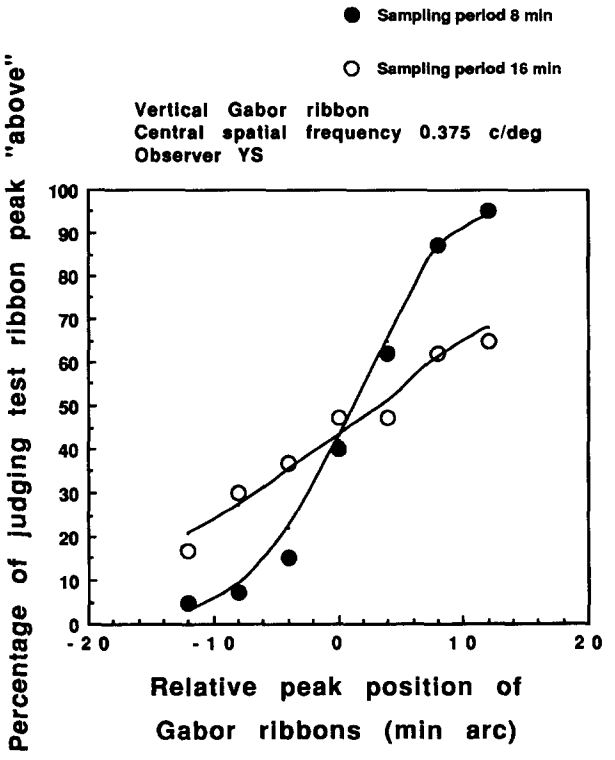

FIGURE 3. Two psychometric functions, one showing more accurate performance (●) than the other (○). The slopes of these functions provide an index of the accuracy of stereoscopic vernier acuity (see text).

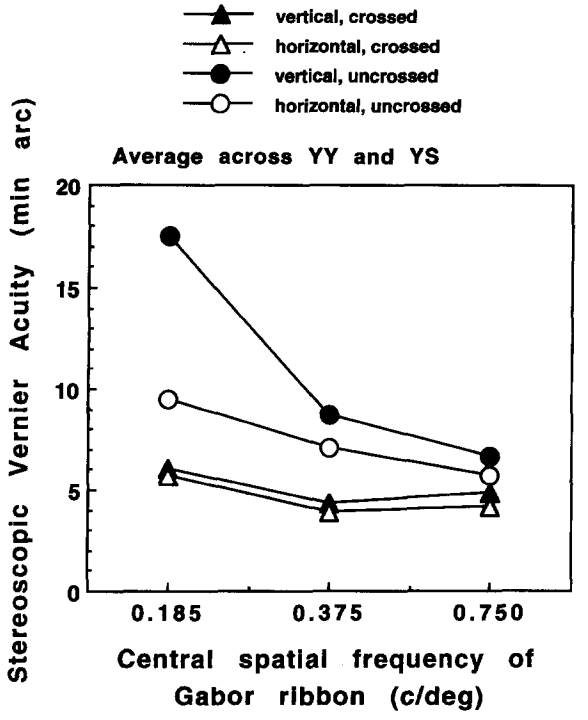

FIGURE 4. Stereoscopic vernier threshold when both ribbons were depicted by smooth, continuous variations in disparity.

cumulative Gaussian, which corresponds to a value of 84% on the psychometric function.)

How accurately can observers locate the peaks in the Gabor ribbons when both surfaces are continuously represented, i.e. when disparity is unsampled? Figure 4 summarizes SVA (i.e. reciprocal of slope, as defined above) for the zero sampling condition as a function of the center spatial frequency of surface curvature. Most obviously, SVA was better for crossed than for uncrossed disparity and tended to be better when the long axis of the surface was horizontal, at least for the uncrossed condition. There is a tendency for SVA to improve with spatial frequency, with this effect being most pronounced for the uncrossed condltions. At their best, observers were able to discriminate the depth peaks in three-dimensional surfaces offset by as little as 4 min arc. Compared to conventional vernier acuity, which can be as little as several sec arc, SVA appears coarse. Note, however, that a value 4 min arc is less than 1.5% of the period of the Gabor ribbon of spatial frequency 0.185 c/deg.

Of more immediate interest is SVA performance when one surface is specified by sampled disparities. Referring to Figs 5 and 6, the three curves in each panel correspond to different spatial frequencies of the Gabor

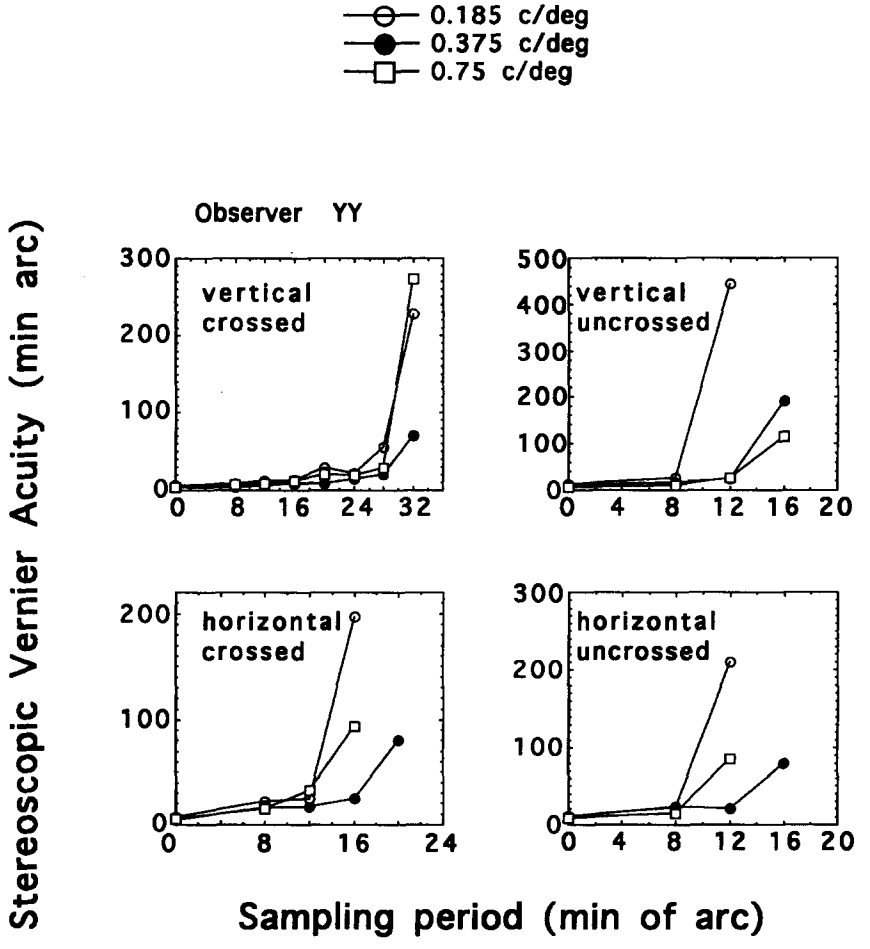

FIGURE 5. Stereoscopic vernier threshold for sampled three-dimensional surfaces. In all graphs the abscissa plots disparity sampling period. Figure inserts indicate the particular conditions. Results are for observer YY. Note the scale differences for various panels in this and the next three figures—if all graphs were plotted using the same scale, the relative positions of data points in some conditions would be obscured.

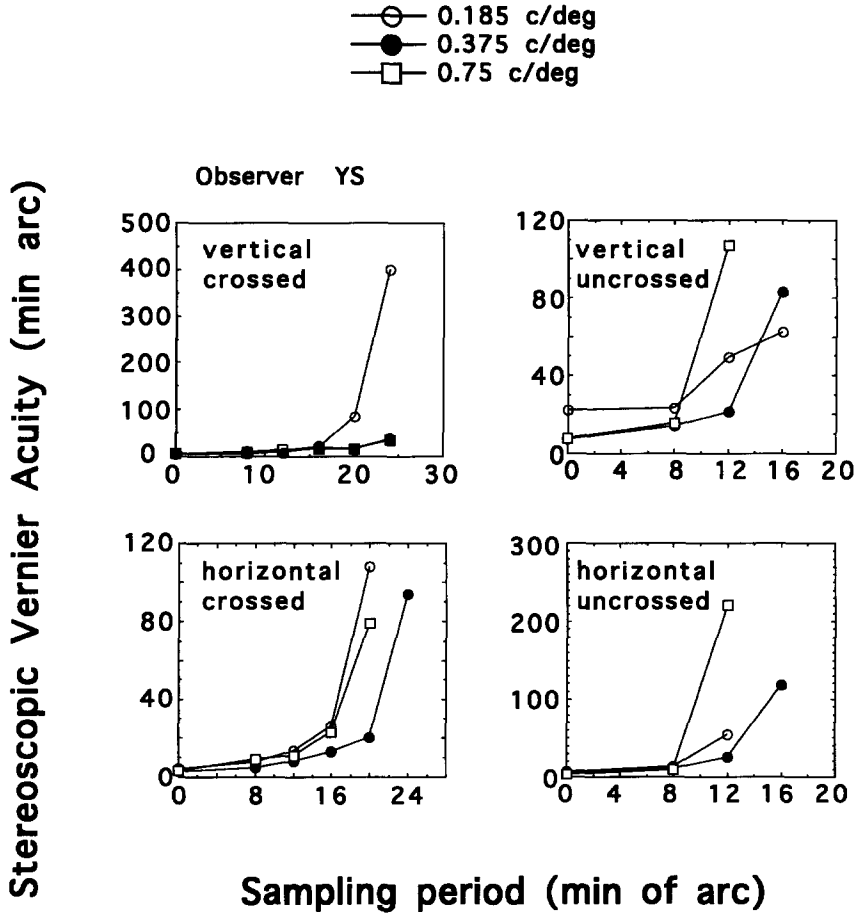

FIGURE 6. Stereoscopic vernier thresholds for sampled three-dimensional surfaces. Results are for naive observer YS.

disparity profile. For all conditions, SVA increased little, if at all, up to a given sampling period, but beyond this value performance deteriorated rapidly. Incidentally, the gaps in the sampled surface were quite obvious to both observers at values of sampling period where their performance was still quite good—visible gaps *per se* did not impair their abilities to interpolate the sampled surfaces. [On average, observers were aware of the sampled surface at periods at and beyond 8 min arc, the disparity sampling reproduced when Figs 1(c) and 2(c) are viewed from the appropriate distance.]

To define the sampling period beyond which interpolation was impossible, we devised the following procedure. First, we assumed that the curves in Figs 5 and 6 consist of two parts, one a linear increase discrimination threshold with sampling period and the other an exponential function. This can be expressed as:

$$T = a + b \times x + a \times (x/p)^m \qquad (1)$$

where T is the function defining changes in SVA with sampling period, x is sampling period, and a, b, p, and m are constants. The constant a represents discrimination performance when the sampling period is zero (i.e. the values in Fig. 4). When the sampling period, x, is $<p$, and if m is very large relative to $a + b \times x$, the term $a \times (x/p)^m$ can be ignored because $(x/p) < 1$. In this case, T is determined almost entirely by the linear component of the equation, $T = a + b \times x$. Thus, b defines the rate of threshold increase when $x < p$. When $x = p$, $T = 2a + bp$. When $x > p$, T increases very rapidly because $(x/p) > 1$ and m, as assumed above, is large. Thus, reasonably, p can be interpreted as the interpolation limit beyond which surface curvature becomes essentially impossible to perceive. (Another way to think about the value p is that it represents a transition point at which the slopes of the psychometric functions abruptly become very shallow.)

A least-squares procedure was used to find values for the constants a, b, m, and p in equation (1) to maximize the fit of equation (1) to the experimental data. Figures 7 and 8 show the best fitting curves superimposed on the original data for both observers. As can be seen, the fits are generally quite close, with r-values all greater than 0.91.

The value p in equation (1) represents the sampling period beyond which SVA increases rapidly, implying that disparity interpolation breaks down. Thus we may take this value as an index of the sampling limit. Figure 9 plots the value p for the different conditions tested in this study. Several points are noteworthy. First, the sampling limit does not vary systematically with spatial frequency of depth modulation (or, in other words, with surface curvature). This is perhaps not surprising, for the spatial frequency values used in our study fall within the range of maximum sensitivity for detection of disparity corrugations (Tyler, 1974; Rogers & Graham, 1982).

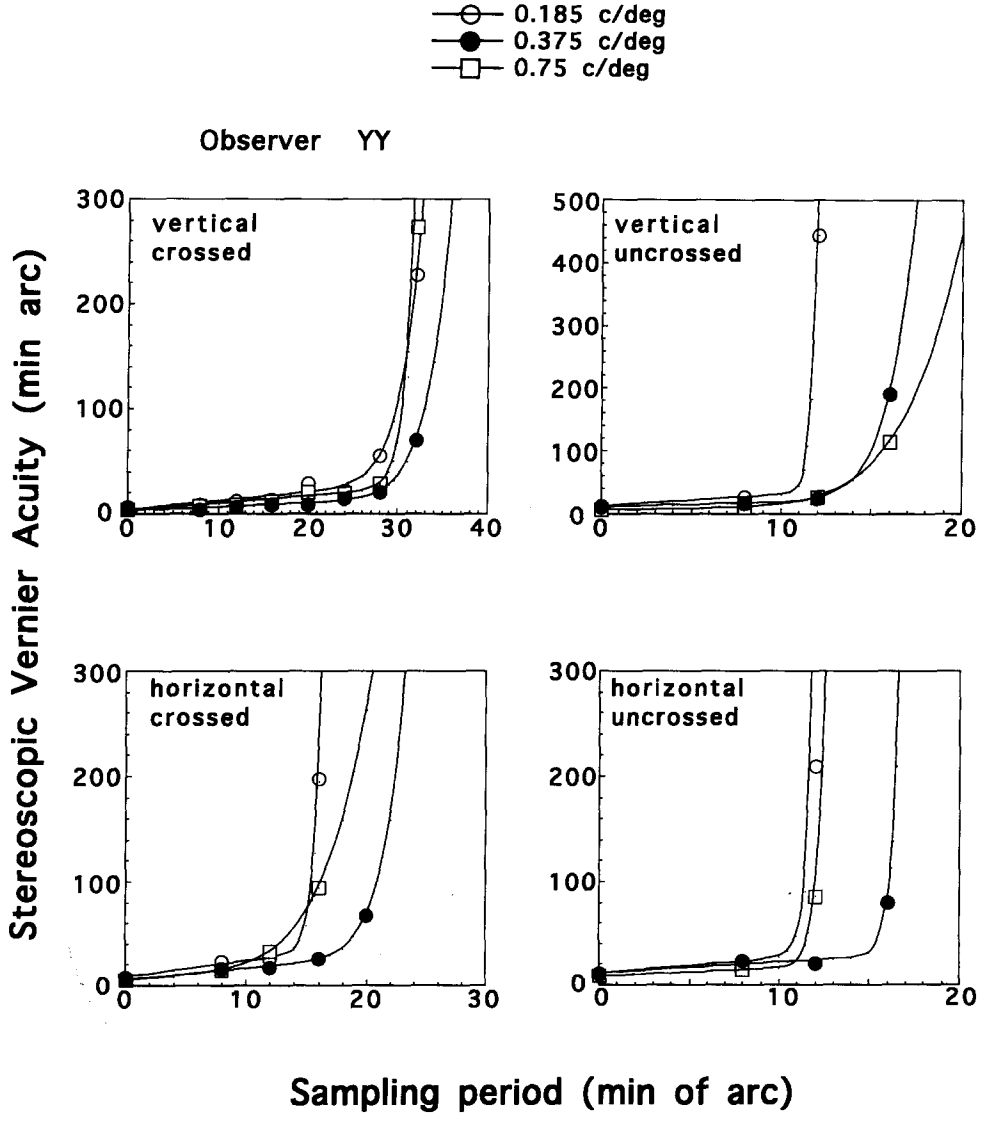

FIGURE 7. Best fitting curves to data shown in Fig. 5.

Evidently the limits of disparity interpolation are unsystematically related to spatial frequency within this range where stereo sensitivity is best. Second, interpolation is possible over coarser sampling periods with crossed disparity than with uncrossed disparity.* This represents yet another instance in which stereo performance differs with the sign of disparity (Mustillo, 1985). Third, and finally, disparity interpolation seems to operate over broader spatial extents when the variation in curvature is along the vertical axis (meaning that the disparity values are constant for any given horizontal band of the surface). This vertical/horizontal anisotropy is reminiscent of other findings in which stereo performance differs for stereoscopic surfaces whose depth modulations are oriented horizontally vs vertically (Parker & Yang, 1988; Rogers & Graham, 1983). We shall return to this last point in the Discussion.

*One referee pointed out that several of the data curves for uncrossed conditions—but none for crossed—contained only three data points (see Figs 5 and 6) and, therefore, the best-fit curves (Figs 7 and 8) for these data are underconstrained. Note, however, that the small number of data points for those uncrossed conditions arises because the task became impossible at larger sampling periods. Thus the conclusion about the difference in interpolation limit between crossed and uncrossed disparities remains valid.

DISCUSSION

Using a novel stereoscopic task, the present experiment reconfirms that the visual system can reconstruct surface properties by interpolating over disparity discontinuities, even when those discontinuities are relatively large (approx. 0.3 deg at the maximum). Beyond a critical value in disparity discontinuity, however, stereoscopic interpolation fails rather abruptly. This failure, incidentally, cannot be attributed to a reduction in the width of the portions of the surface explicitly specified by disparity, for in fact, this width remained constant (i.e. 4 min arc) and only the spacing of that explicit disparity information varied. (Of course, the percent of the entire Gabor ribbon explicitly defined by disparity varied inversely with sampling period.) Moreover, we are confident that observers were not simply performing the judgment based on the location of the

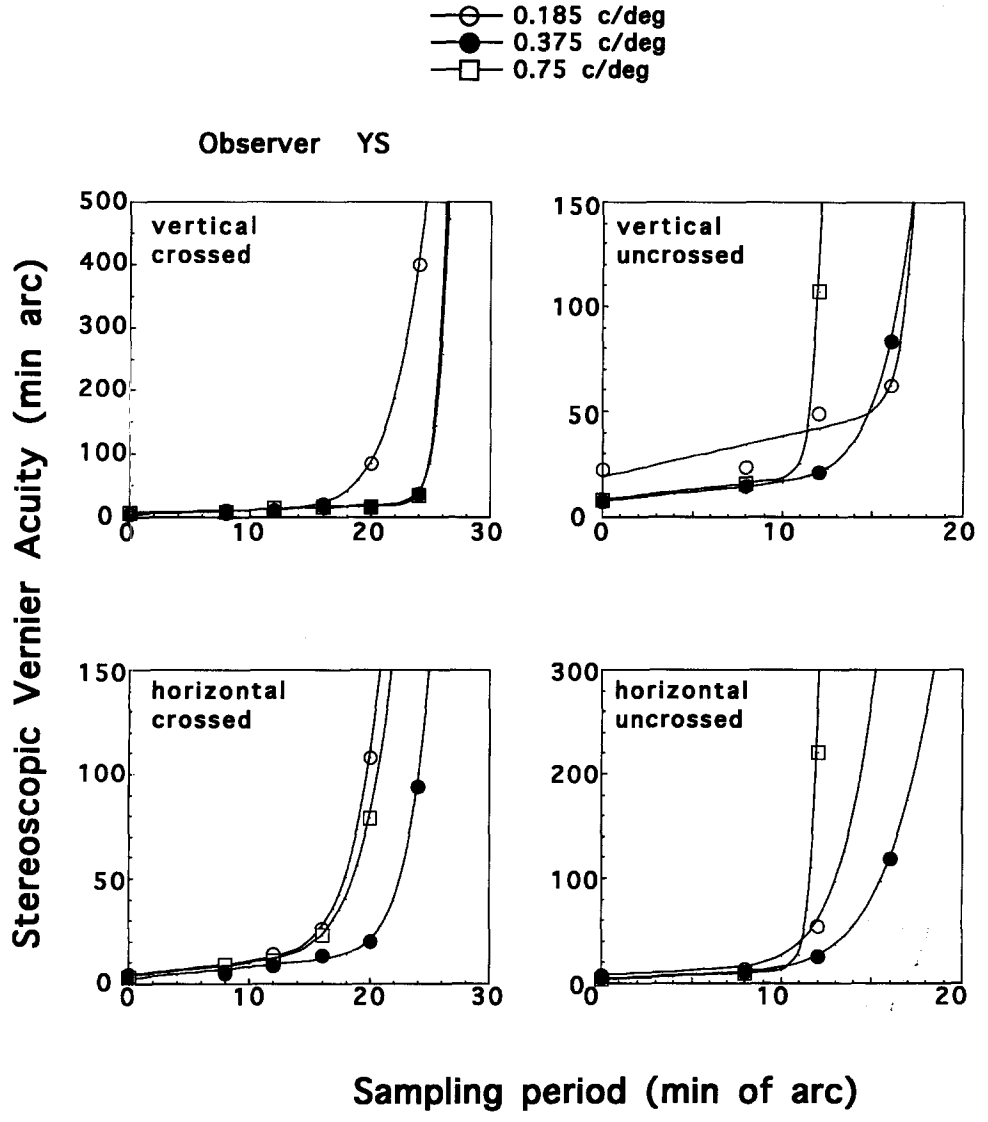

FIGURE 8. Best fitting curves to data shown in Fig. 6.

largest disparity value explicitly represented in the target, for those explicit peaks did not necessarily correspond to peaks in the Gabor ribbons. And if observers were basing their judgments on explicit disparity peaks, SVA should not have been smaller than one sampling period, yet in many conditions SVA was smaller than this. We conclude that observers based their judgments on the positions of the peak of the interpolated Gabor surface, not the position of the sample with maximum disparity.

It is noteworthy that the interpolation limit (i.e. the sampling period beyond which interpolation rapidly disintegrates—see Fig. 9) is unrelated to the spatial frequency of the depth modulation (i.e. to the space constant of the Gabor function), at least within the two-octave range tested in our work. Based on the sampling theorem (Brigham, 1974), one would predict that the upper limit of disparity sampling should vary inversely with the spatial frequency of depth modulation, since accurate reconstruction of a surface requires sampling at a frequency that is at least one-half of the highest spatial frequency represented in the stimulus. The data do not conform to this prediction, implying that successful surface interpolation from disparity depends primarily on the spatial extent of the disparity samples. This conclusion must be tempered, however, by the specifics of our displays. Strictly speaking, the sampled ribbons consisted of periodic regions where disparity was zero [refer to Fig. 1(d)], not where disparity information was missing.

Periodic disparity modulations of a three-dimensional surface are visible at spatial frequencies up to 5 c/deg, with modulations beyond this limit blurring together into a uniform surface (Tyler, 1974; Schumer & Ganz, 1979; see also Parker & Yang, 1989). In this sense, the stereoscopic system behaves like a low-pass filter in the disparity domain. Consistent with this aspect of stereo vision, observers in our experiment were unable to perceive the periodic interruptions in the Gabor ribbons when the sampling period was 8 min arc or less. (Recall, though, that our disparity modulations, while periodic, involved unequal duty cycle.) Moreover, when sampling *was* sufficiently coarse to be perceived, observers described the surfaces of those ribbons as smooth and well-defined, for sampling periods up to 16 min arc.

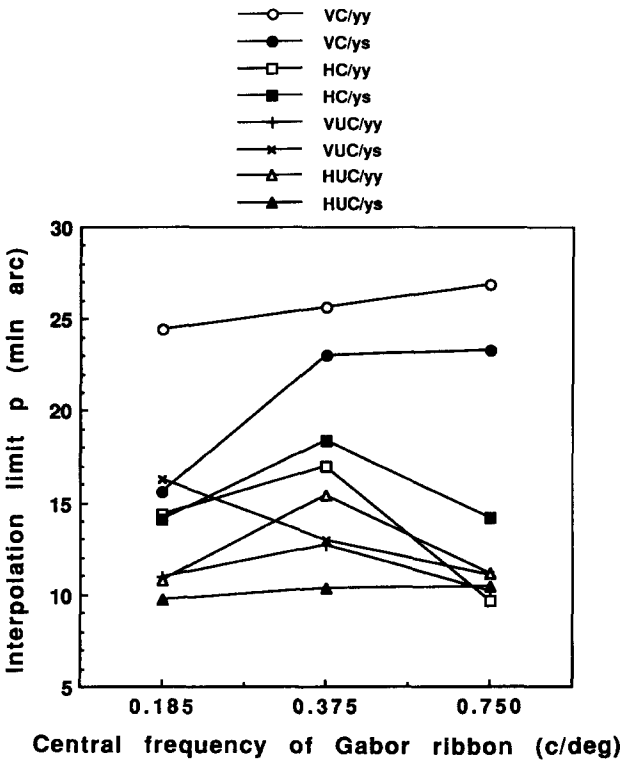

FIGURE 9. Interpolation limit [defined by value p in equation (1)] as a function of Gabor center spatial frequency. The legend symbols denote the observer (YY and YS), the Gabor ribbon orientation (V and H), and the sign of the disparity (UC and C).

In this sense, the stereo ribbons resembled surfaces defined by illusory contours—interpolated contours were smooth even though inducing elements were noticeably discrete.

Based on these observations, one could conclude that the smooth, continuous surface is registered by neural units responsive to low spatial frequency modulations in disparity (i.e. broad depth curvature) while, at the same time, the visible disparity discontinuities are registered by units responsive to disparity modulations at higher spatial frequencies. The existence of such units has been proposed by Lehky and Sejnowski (1990), whose neural model of stereopsis is populated by neurons whose breadth of disparity tuning varies with preferred disparity. In particular, their model assumes that units maximally responsive to large disparities are more broadly tuned for disparity than are those responsive to small disparities. The units more broadly tuned to disparity would respond preferentially to low frequency modulations in disparity, and the more narrowly tuned units would respond best to higher frequency modulations in disparity. To the extent that this model is correct, we propose that it is the broadly tuned units that are responsible for disparity interpolation, whereas the more narrowly tuned units are at the same time signaling the visible discontinuities in disparity.

Some investigators (e.g. Rogers & Cagenello, 1989) have proposed that the visual system might compute something like the second spatial derivative of disparity—i.e. disparity curvature. This theory predicts that surface reconstruction should be more accurate for vertically oriented Gabor ribbons (see Rogers & Graham, 1983). This anisotropy indeed was observed in our data. It should be noted, however, that a vertical/horizontal anisotropy in our task could also be explained without appeal to disparity curvature, simply by assuming that local disparity signals arising from neighboring surface regions are pooled, with the extent of pooling being greater in the horizontal dimension.

Surface interpolation from discretely sampled disparities is one instance of a class of phenomena all involving spatial interactions in the determination of perceived depth from disparity. In these final paragraphs, we briefly describe some of these other depth phenomena, pointing out where possible the similarities to our results.

Perhaps the simplest form of depth interpolation occurs when one dichoptically views a pair of rectangles differing slightly in width (e.g. Ogle, 1950). One experiences a single rectangle rotated in its entirety—intervening homogenous region and all—about the vertical axis. A comparable "capture" effect has been described by Ramachandran (1986) using disparate figures created from illusory contours. These kinds of demonstrations certainly constitute evidence for interpolation, for disparity is explicitly specified only at the left and right edges. What happens, though, when the space betwen lateral edges is filled with surface markings of some sort? The answer seems to depend on several things, as the following results imply.

Mitchison and McKee (1985, 1987a) had observers view stereograms composed of a horizontal row of regularly spaced dots, with the dots at the left and right edges of the display given some explicit disparity value(s). Even though the disparity of the repetitive, intermediate dots was ambiguous (because of the multiple possible matches), the perceived plane of depth of these dots corresponded to an imaginary plane connecting the two end dots. This spread of disparity from the end dots only occurred with dot spacings $\leqslant$ 5–7 min arc. (Note, however, that the two end dots putatively promoting this interpolation process were themselves separated by over 1 deg.) So within spatial limits, unambiguous disparity signals may induce a particular depth on binocularly ambiguous repetitive elements. This induction of depth within ambiguous regions may also apply to stereoscopic slant occurring when the two eyes view vertical gratings differing slightly in spatial frequency (Blakemore, 1970) but evidently does not apply to tilt from illusory contours (Ramachandran, 1986). It is worth noting that in our work with Gabor ribbons, evidence for successful interpolation was found for intersample distances ranging from 10 to 25 min arc, depending on conditions (recall Fig. 9); these limiting values are far in excess of those reported by Mitchison and McKee. Our stereo targets, however, were much more richly textured than those employed by Mitchison and McKee, and our disparity was large relative to their's.

Collett (1985) examined depth interpolation using

RDSs that included an exclusively monocular portion (i.e. regions where only one half-image contained dots) situated next to or within binocular portions (i.e. regions where both half-images contained dots specifying particular disparities). Even though the monocular region contained no explicit information for depth, observers could perceive a surface whose shape and depth were determined by the depth and orientation of the adjacent binocular regions. For instance, when placed between two binocular rectangles imaged at different disparities (and hence seen at different depths), an interpolated monocular region appeared as a slanted plane interconnecting the two binocular regions. In his studies, Collett always used abutting monocular and binocular regions, and perceived depth in the monocular region fell off with distance from the nearest binocular edge. In an interesting twist on Collett's experiment, Buckley, Frisby and Mayhew (1989) found that sharp texture boundaries in a monocular region could influence the perceived three-dimensional surface interpolated between regions specified by disparity. In fact, sharp monocular texture boundaries could completely override smooth disparity interpolation.

Wurger and Landy (1989) obtained depth judgments using RDSs in which a central region was either uniform or contained texture; the lateral separation between the vertical edges of this region carrying explicit disparity information was 2.7 deg. Evidence for interpolation was found, in that perceived depth within the central, ambiguous region varied monotonically from one edge of the region to the other. Paradoxically, depth was degraded when the actual disparities at the edges of the central region were large. Interpolated depth was also sharply degraded when the two regions contained textures that were uncorrelated (i.e. rivalrous) between the two eyes. In other contexts, too, rivalry has been shown to disrupt stereopsis (Blake, Yang & Wilson, 1991; Frisby & Mayhew, 1978).

In the disparity interpolation work described so far, sparsely textured or ambiguous regions appear as complete surfaces—in other words, areas lacking explicit disparity information acquire their depth from neighboring regions where disparity information is present. A complementary situation occurs when regions of a stereogram contain two (or more) sets of explicit disparity values that each, on its own, specify a given depth plane. When those disparities specify planes very close in three-dimensional space, observers in fact perceive a single surface situated midway between the separate depth planes—this effect implies disparity averaging (e.g. Parker & Yang, 1989) and it occurs only for disparities within about 0.5 min arc of one another. As the difference in disparity between planes grows beyond this value, the single plane appears to thicken—an effect termed pyknostereopsis (Tyler, 1983)—and then to break into multiple, individual depth planes overlaying one another—stereo transparency (e.g. Weinshall, 1989). In these instances of averaging, thickening and transparency, disparity interactions occur within the z-axis (i.e. the depth axis). Lateral disparity interactions have also been described. Using dots and lines as stereo targets, Westheimer (1986) reported that the depth of one stimulus element may be pulled toward the depth of another, closely spaced element. Once the separation between elements exceeds about 3 min arc, this "attraction" effect gives way to "repulsion" whereby the depth between neighboring elements is exaggerated. This 3 min arc transition value, incidentally, compares favorably with the upper limit of resolution for disparity modulated RDS patterns (Tyler, 1974; Parker & Yang, 1989).

The phenomena discussed in this section all represent instances of disparity interaction. It may be useful to distinguish, however, between disparity propagation (attraction, repulsion and averaging) and disparity interpolation. In the case of the former, perceived depth from disparity is influenced by neighboring disparity values—for central vision, these kinds of disparity interactions occur within a rather limited spatial extent. In the case of the latter, surface shape is reconstructed or completed from coarsely sampled disparities—interpolation may occur over rather large spatial extents. It is noteworthy, too, that fairly accurate surface completion is possible even when the disparity samples are so coarse as to be visible. Disparity interpolation seems to operate to recover three-dimensional surface shape, not just modify depth associated with a given disparity.

REFERENCES

Blake, R., Yang, Y. & Wilson, H. (1991). On the coexistence of stereopsis and binocular rivalry. *Vision Research, 31*, 1191–1204.

Blakemore, C. (1970). A new kind of stereoscopic vision. *Vision Research, 10*, 1181–1199.

Brigham, E. O. (1974). *The fast Fourier transform*. Englewood Cliffs, N.J.: Prentice Hall, Inc.

Buckley, D., Frisby, J. P. & Mayhew, J. E. W. (1989). Integration of stereo and texture cues in the formation of discontinuities during three-dimensional surface interpolation. *Perception, 18*, 563–588.

Collett, T. S. (1985). Extrapolating and interpolating surfaces in depth. *Proceedings of the Royal Society of London, B 224*, 43–56.

Fox, R. & Oross III, S. (1988). Deficits in stereoscopic depth perception by mildly mentally retarded adults. *American Journal on Mental Retardation, 93*, 232–244.

Frisby, J. P. & Mayhew, J. E. W. (1978). The relationship between apparent depth and disparity in rivalrous-texture stereograms. *Perception, 7*, 661–678.

Julesz, B. (1971). *Foundation of cyclopean perception*. Chicago: University of Chicago Press.

Lehky, S. R. & Sejnowski, T. J. (1990). Neural model of stereoacuity and depth interpolation based on a distributed representation of stereo disparity. *Journal of Neuroscience, 10*, 2281–2299.

Mitchison, G. J. & McKee, S. P. (1985). Interpolation in stereoscopic matching. *Nature, 315*, 402–404.

Mitchison, G. J. & McKee, S. P. (1987a). Interpolation and the detection of fine structure in stereoscopic matching. *Vision Research, 27*, 295–302.

Mitchison, G. J. & McKee, S. P. (1987b). The resolution of ambiguous stereoscopic matches by interpolation. *Vision Research, 27*, 285–294.

Morgan, M. J. & Watt, R. J. (1982). Mechanisms of interpolation in human spatial vision. *Nature, 299*, 553–555.

Mustillo, P. (1985). Binocular mechanism mediating crossed and uncrossed stereopsis. *Psychological Bulletin, 97*, 187–201.

Ogle, K. N. (1950). *Researches in binocular vision*. Philadelphia, Pa: Saunders.

Parker, A. J. & Yang, Y. (1988). Investigation of the ordering constraint in human stereo vision. *Perception, 17*, 384.

Parker, A. J. & Yang, Y. (1989). Spatial properties of disparity pooling in human stereo vision. *Vision Research, 29*, 1525–1538.

Ramachandran, V. S. (1986). Capture of stereopsis and apparent motion by illusory contours. *Perception & Psychophysics, 39*, 361–373.

Rogers, B. & Cagenello, R. (1989). Disparity curvature and the perception of three-dimensional surfaces. *Nature, 339*, 135–137.

Rogers, B. & Graham, M. (1982). Similarities between motion parallax and stereopsis in human depth perception. *Vision Research, 22*, 261–270.

Rogers, B. J. & Graham, M. E. (1983). Anisotropies in the perception of three-dimensional surfaces. *Science, 221*, 1409–1411.

Schumer, R. & Ganz, L. (1979). Independent stereoscopic channels for different extents of spatial pooling. *Vision Research, 19*, 1303–1314.

Tyler, C. W. (1974). Depth perception in disparity gratings. *Nature, 251*, 140–142.

Tyler, C. W. (1983). Sensory processing of binocular disparity. In Schor, C. M. & Ciuffreda, K. J. (Eds), *Vergence eye movements: Basic and clinical aspects*. Boston, Mass.: Butterworths.

Weinshall, D. (1989). Perception of multiple transparent planes in stereo vision. *Nature, 341*, 737–739.

Westheimer, G. (1986). Spatial interaction in the domain of disparity signals in human stereoscopic vision. *Journal of Physiology, 370*, 619–629.

Wurger, S. M. & Landy, M. S. (1989). Depth interpolation with sparse disparity cues. *Perception, 18*, 39–54.

Acknowledgements—We thank Heidi Wiesenfelder, Deborah Mauk and Scott Stevenson for commenting on an earlier draft. This work was supported by NIH grant EY07760 and by NIH core grant EY08126.